Journal Pre-proof

Effectiveness of a novel UV light emitting diode based technology for the microbial inactivation of *Bacillus subtilis in model food systems*.

Laura M. Hinds, Clémentine M.G. Charoux, Mahbub Akhter, Colm P. O'Donnell, Brijesh K. Tiwari

PII:	S0956-7135(19)30499-2
DOI:	https://doi.org/10.1016/j.foodcont.2019.106910
Reference:	JFCO 106910
To appear in:	*Food Control*
Received Date:	14 July 2019
Accepted Date:	20 September 2019

Please cite this article as: Laura M. Hinds, Clémentine M.G. Charoux, Mahbub Akhter, Colm P. O' Donnell, Brijesh K. Tiwari, Effectiveness of a novel UV light emitting diode based technology for the microbial inactivation of *Bacillus subtilis in model food systems*., *Food Control* (2019), https://doi.org/10.1016/j.foodcont.2019.106910

Effectiveness of a novel UV light emitting diode based technology for the microbial inactivation of *Bacillus subtilis in model food systems*.

Laura M. Hinds[1,2] , Clémentine M. G. Charoux[1,2], Mahbub Akhter[3], Colm P. O'Donnell[2] and Brijesh K. Tiwari[1,2]

[1]Food Chemistry & Technology, Teagasc Food Research Centre, Dublin, Ireland
[2]School of Biosystems and Food Engineering, University College Dublin, Dublin, Ireland
[3]Senior Process Architect, Lumentum, Caswell, NN12 8EQ, UK

Address for correspondence: Teagasc Food Research Centre, Ashtown, Dublin, Ireland.; Tel: +35318059722; Email: laura.hinds@ucdconnect.ie

ABSTRACT

The objective of this study was to assess the effectiveness of a novel UV multiwavelength light emitting diode (LED) based technology for the inactivation of *B. subtilis* in two model food systems. The LED based system was used to treat *B. subtilis* bacterial cultures using various combinations of UV wavelengths (285, 365, 405, 285/365, 285/405, 365/405, 285/365/405 nm) for different treatment durations (5 & 10 min). Bacterial enumerations, post-treatment analysis and SEM imaging were carried out. UV treatment at 285 nm was found to be the most efficient individual wavelength for inactivation resulting in > 6 $\log_{10}$ reductions. Treatments at other wavelengths investigated also resulted in bacteriostatic effects. Synergistic effects were observed for treatment at a 285/405 nm combination in one model system. Growth kinetics were carried out using a modified Gompertz model and model fit was assessed by root mean squared error, accuracy factor and bias factor. Experimental data showed good fit with model employed with RMSE values ranging from 0.01 x 10^{-2} to 1.367 x 10^{-2} for 5 min treatment, and 0.01 x 10^{-2} to 0.210 x 10^{-2} for 10 min treatment. Multivariate analysis was also carried out using principal component analysis and explained 100% of the variation observed for 3 principal components. This study shows that UV-LED technology is effective as bactericidal and bacteriostatic technology, depending on wavelength used.

1. Introduction

Conventional heat or chemical based techniques in food processing can induce adverse effects in food products, leading to loss of desired organoleptic properties and damage to temperature liable nutrients and vitamins (Cullen, Tiwari, & Valdramidis, 2012). Furthermore, thermal processes (pasteurization, sterilization, evaporation, refrigeration, freezing, and drying) are among the most energy-consuming technologies in the food industry (Picart-Palmade, Cunault, Chevalier-Lucia, Belleville, & Marchesseau, 2019). Alternative non-thermal processing technologies are continuously being developed in the food industry to ensure safe, high quality food with sufficient shelf life while also having minimal environmental impacts. While ultraviolet light has been employed commercially as a disinfection technology for water treatment and as a sterilisation technique in the medical field for many years, investigation of the potential of this technique in the food industry has only recently commenced.

Ultraviolet (UV) light is electromagnetic radiation within the wavelength range of 10 to 400 nm, in between x-ray and visible wavelengths. It is often referred to as non-ionising radiation; however, the shortest wavelengths emit some ionisation (Sandle, 2013). The UV spectrum is sub-divided based on various wavelengths and applications. Sub-divisions widely used in

the scientific literature include: UVA (315 – 400 nm), UVB (280 – 315 nm) and UVC (<280 nm) (Soni, Oey, Silcock, & Bremer, 2016). Wavelengths below 200 nm are classified as vacuum ultraviolet. UV light has been demonstrated to be successful for the inactivation of pathogenic bacteria in liquid foods and water (Akgün & Ünlütürk, 2017; Song, Mohseni, & Taghipour, 2016). Microbial inactivation is achieved with minimal loss of nutritional and sensorial qualities of food and no known toxic effects or residues (Gayán, Condón, & Álvarez, 2014).

The primary mechanism by which microorganisms are inactivated by UV light is *via* genetic interference, although other cell components such as proteins can also be affected (Gayán, et al., 2014). Microbial inactivation using UV light occurs through various mechanisms that are dependent on the wavelengths applied in treatment and can be achieved directly, by absorption of the incident light on microbial cell DNA initiating dimer formation, or indirectly, due to generation of reactive oxygen species by the interaction of radiation with cellular chromophores acting as photosensitisers (Brem, Guven, & Karran, 2017; Kim, Kim, & Kang, 2017). The UVC range, also termed the germicidal range, is the most effective range for microbial inactivation, due to the peak of maximum effectiveness corresponding with the peak of maximum DNA absorption.

There are multiple sources of ultraviolet light that are commercially applied worldwide. However, these sources which are primarily mercury lamps are unsustainable, and have multiple drawbacks including high energy requirements and production of harmful waste. Light emitting diodes (LEDs) are an excellent alternative source of UV light due to their lower energy requirements, longer life span, zero waste production and minimal heat generation. LEDs are two-terminal semiconductor devices, which emit light under forward bias conditions. Different semiconductor materials emit different colours (wavelengths) of light; the emission wavelengths are dependent on the semiconductor band gap of the material. Positively charged carriers (holes) in the p-type layer are driven towards the active (junction) layer where they recombine with electrons which are driven by the same bias from the n-type layer in the opposite direction towards the junction. When the electron and hole meet, they recombine under emission of a photon which removes the energy that is released upon recombination.

The objective of this paper is to investigate the effectiveness of a novel UV light emitting diode based technology for the microbial inactivation of *Bacillus subtilis* in model food systems.

2. Material and Methods

2.1. Chemicals and reagents

Peptone buffered saline (BR0014G), maximum recovery diluent (CM0733B), nutrient agar (CM0003B) and nutrient broth (CM0001B) were purchased from Fannin Ltd (Ireland). Glutaraldehyde (G5882), ethanol and hexamethyldisilazane (440191) were purchased from Sigma Aldrich (Ireland).

2.2. Experimental set up

A multiwavelength LED based system was fabricated in collaboration with Ndevices Ltd, Co. Cork, Ireland. The system comprised of a three channel LED conditioner, enabling precise control of LEDs (3 x 3 LEDs; 3 x NVSU233A-U365 LG Innotek and 3 x LEUVA66B00HF00 and 3 x NCSU275T, Nichia Corporation) emitting at 285, 365 and 405 nm. Spectra were obtained using an Ocean Optics USB2000 spectrometer .and each LED channel comprised of 3 LEDs in series placed in an optimized pattern (Fig 1). The LEDs were mounted on an aluminium heatsink equipped with a cooling fan. All wavelengths were used individually or in combination as follows: 285, 365, 405, 285/365, 285/405, 365/405and 285/365/405 nm in all experiments. All LEDs were used at their maximum amperage. The distance between the LED-UV source and samples was set at 1 cm for all experiments. Samples (3 mL) were placed in petri dishes (5.5 cm diameter) and all treatments were carried out for two exposure times (5 and 10 min) at room temperature. All experiments were carried out in triplicate.

2.3. Microbiological strains and growth conditions

Bacillus subtilis DSM 618 (Merck, Germany) was inoculated into 25 ml nutrient broth (24 h at 30ºC). Bacteria were washed by centrifugation (6, 000 x g) and pellets were resuspended in PBS (pH 7.2), for PBS model.

2.4. Bacterial enumeration

Plate counting was carried out on all samples (treated and non-treated control) by serially diluting (1 mL) in maximum recovery diluent (9 mL) then 0.1 mL of corresponding dilutions were plated on nutrient agar, in duplicate. After incubation at 30°C for 24 h, colonies were counted. Counts of bacterial colonies on NA plates were expressed in cfu/mL. All experiments were carried out in triplicate.

2.5. Growth curve conditions.

The growth of non-treated and UV LED treated *B. subtilis* was monitored by measuring optical density (OD) of each sample (serially diluted in a 96 well plate), at a wavelength of 600 nm at 30ºC over the 24 h incubation period using spectrophotometer (Epoch 2 microplate spectrophotometer, BioTek, USA). Enumerations of *B. subtilis* cultures were carried out directly after treatment by plate count in duplicate. Primary growth model

parameters of specific growth rate (μ_{max}, h^{-1}) and lag phase (λ, h) were obtained to evaluate the growth curve by fitting OD_{600nm} versus incubation time to the modified Gompertz model (Equation 1) using the DMFit excel based tool (Baranyi & Roberts, 1994).

$$OD_t[-] = OD_0 + \frac{[OD_{max} - OD_0]}{[1 + e^{(-B(t-M)}]} \quad [1]$$

$$\mu_{max}[h^{-1}] = \frac{[OD_{max} - OD_0]}{e} \times B \quad [2]$$

$$\lambda[h] = M - \frac{1}{B} \quad [3]$$

OD_0 and OD_{max} are the initial and maximum optical density [-]; OD_t is the optical density at incubation time (h); *B* is the maximum relative growth (h^{-1}) at *t=M* and *M* is the time (h) at which the absolute growth rate was at a maximum and "*e*" is the base for natural logarithm.

2.6. Scanning electron microscopy

The morphological structure of UV LED treated and non-treated *B. Subtilis* cells were visualised using a scanning electron microscope (FEI Quanta 3D FEG DaulBeam, FEI Ltd, USA). Cell preparation was performed according to E. Fratesi, L. Lynch, L. Kirkland, and R. Brown (2004), with modifications. Samples were mounted on stubs using double-sided carbon tape, and sputter coated with Gold, using an Emitech K575X Sputter Coating Unit, to prevent surface charging by the electron beam.

2.7. Statistical analysis

All experiments were carried out in triplicate and average values reported. Analysis of variance (ANOVA) and Tukey's test was carried out using SAS (Version 9.4). Mean values were considered significant at $P<0.05$. PROC CORR procedure of SAS was carried out to investigate correlations between all parameters. Goodness of model fit was analysed based on coefficient of regression (R^2), root mean squared error (RMSE), residual analysis, accuracy factor and bias factor were calculated using experimental vs predicted OD values fitted to modified Gompertz model.

$$RMSE = i = 1(ODEi - ODP)2nt - np \quad [4]$$

$$AF = 10i = 1(log10ODP - log10ODe)2n \quad [5]$$

$$BF = 10i = 1(log10ODP - log10ODe) \quad [6]$$

Where

OD_E is the experimental OD

OD_P is the model predicted OD value

n_t is the number of data points

n_p is the number of estimated model parameters

n is the number of experimental measurements

3. Results and Discussion

3.1. B. subtilis inactivation

Inactivation of *B. subtilis* vegetative cells by the UV LED light system is shown in Fig. 2 and 3. Fig. 2 (i-iii) shows the effect of UV wavelength (285, 365, 405 nm) for 5 and 10 min treatment times on microbial inactivation of vegetative cells of *Bacillus subtilis*. A significant reduction of 6.82±0.09 $\log_{10}$ i.e. complete inactivation was observed at 285 nm, for both treatment times, when exposed to UV wavelength in a peptone buffered saline (PBS) solution whereas a significant reduction of 3.58±0.33 $\log_{10}$ was observed in the case of nutrient broth (NB). The lower inactivation in NB could be attributed to suspended solids in the media which interfered with the absorption of light and therefore resulted in a lower inactivation efficiency (Guerrero-Beltran & Barbosa-Canovas, 2006). Similarly, Song, Taghipour, and Mohseni (2019) achieved significant inactivation (2.8 $\log_{10}$) in a PBS model solution at 285 nm for *E. coli*. While this was a lower inactivation value in comparison to the current study, a much shorter exposure time of 40 s was employed for these treatments. Akgün and Ünlütürk (2017) investigated the potential synergistic effects of various UV wavelengths (254, 280, 365, 405) in the inactivation of *E. coli* K12 in both cloudy and clear apple juice. The most effective individual treatment wavelength was 280 nm, achieving a 4.40 $\log_{10}$ reduction after a 40 min treatment time. Combined treatment wavelengths of 280/365 achieved a lower reduction of 3.9 $\log_{10}$ for the same treatment time. The results in the current study are consistent with those of Akgün and Ünlütürk (2017) who reported that higher inactivation was observed in clear apple juice than cloudy apple juice. The lower inactivation observed in cloudy apple juice was attributed to colour compounds, organic matter, and suspended solids in the juice. No significant reduction was obtained at either 365 (0.17±0.21 – 0.69±0.40 $\log_{10}$) or 405 nm (0.07±0.09 – 0.12±0.08 $\log_{10}$) irrespective of the growing media or treatment time. These wavelengths reside in the UVA region of the spectrum which is included in the photoreactivation light range of 300-500 nm (Song, et al., 2019).

Fig. 3 (i-iv) shows the treatment effect of various combinations of UV wavelength (285/365, 285/405. 365/405 and 285/365/405 nm) on *B. subtilis* for both PBS and NB. It can be

observed that complete inactivation (6.82±0.09 log_{10} cfu/mL) was achieved after exposure to 285/365 nm and 285/365/405 nm wavelength combinations after 5 min of treatment time in PBS solution whereas, significant reductions of 5.39±1.19 log_{10} were achieved for combinations of 285/405 nm after 5 min and 6.27±0.08 log_{10} after 10 min. Lower efficacy was observed in the case of NB for wavelength combinations, with 285/365/405 being the most effective showing reductions of 2.17±0.45 log10 and 4.05±1.14 log_{10} for 5 and 10 min, respectively. Fig. 2 shows that treatment at the individual wavelength of 285 nm alone achieved complete inactivation, highlighting no synergistic effects for treatment at the 285/405 nm combination. Previous studies have reported a significantly higher inactivation of bacteria treated at selected wavelength combinations (280/365 and 280/405 nm) than at an individual wavelength (280 nm) (Chevremont, Farnet, Coulomb, & Boudenne, 2012; Chevremont, Farnet, Sergent, Coulomb, & Boudenne, 2012). Similar observations were observed in this study in the case of NB but not in the case of PBS. This is because complete inactivation was observed with PBS whereas significantly lower inactivation was observed for NB. However, log_{10} reductions of 2.13±1.19 and 3.89±0.87 for 5 and 10 min treatment time with 285/405 nm, respectively, were observed in NB, in comparison with individual wavelength (285 nm) treatments alone for this model, which achieved log reductions of 1.89±0.16 and 3.57±0.33 for 5 and 10 min, respectively; thus showing an additive or synergistic effect. Fig. 4 shows an SEM image of *B. subtilis* cells in NB, before and after exposure at 285 nm. In comparison to the non-treated control, the cells exposed to UV light have altered surface morphologies, highlighting the germicidal effects of this treatment wavelength.

No significant reductions (0.05±0.14 – 0.82±1.10 log_{10}) were obtained in either model solution for treatment at a wavelength combination of 365/405 nm for both treatment times, indicating that this treatment wavelength may not provide efficient decontamination characteristics to inactivate *B. subtilis*. Some previous studies have reported bacteria log reductions after exposure to UVA radiation, however these studies applied much longer treatment times in comparison to the current study (Aihara, et al., 2014; Lui, Roser, Corkish, Ashbolt, & Stuetz, 2016).

3.2. Growth kinetics

Fig. 5 (i-vii) shows the growth curves obtained for vegetative cells of *B. subtilis* subjected to various treatments, varying in wavelength and durations (5 & 10 min) after 18 h incubation (30°C). The optical density at 600 nm versus incubation time, for different UV treatments (wavelength and time) in PBS solution, was fitted to the Gompertz model. The primary growth kinetic parameters of *B. subtilis* following treatment i.e. specific growth rate and lag phase (λ, h) determined using Equation 1 – 3 are shown in Table 1. The initial optical density

value (Y_0) ranged between 0.084 and 0.085 for all treatments. The coefficient of regression (R^2) was higher than 0.91, except for those values where the model did not fit due to absence of growth. μ_{max} (h^{-1}) and λ (h) for untreated samples were 1.06±0.31 and 2.90±2.00, respectively. No growth i.e. negative μ_{max} was obtained for *B. subtilis* at wavelengths of 285, 285/365, 285/405 and 285/365/405 nm with no λ. Fig. 5 (i, iii, vi) shows growth kinetics of both treatment times for 365, 405 and 365/405 nm wavelengths. μ_{max} (h^{-1}) and λ (h) values for these samples ranged between 1.09 – 1.39 h^{-1} and 4.18 – 7.39 h, respectively. The highest μ_{max} (h^{-1}) value and shortest lag time were obtained for treatment at 405 nm for 10 min duration. It should be noted that the μ_{max} obtained by fitting these models is only a potential rate because, theoretically this exact rate cannot be obtained due to the applied limiting functions which has effects even in the linear phase of the growth curve. However, the difference between the actual rate and rate obtained by the model is negligible if the m_{Curve} curvature parameter obtained from the model fit is sufficiently large (Baranyi & Roberts, 1994). To the best of the authors' knowledge this is the first study to report the growth kinetics of *B. subtilis* vegetative cells treated by various UV LED treatments. From this analysis it can be seen that no repair or photoreactivation occurred after treatment over 18 h incubation period. This highlights the efficiency of these wavelength treatments. It can also be observed, that while UVA wavelengths were not sufficient to significantly reduce microbial load, there was an increase in bacteriostatic effects with longer treatment times at these wavelengths.

3.3. Model fitting

The Gompertz model is a growth curve with sigmoidal function commonly used to describe the behaviour of micro-organisms under different treatments. The Gompertz model is often used for its flexibility and asymmetrical sigmoid shape compared to other linear models such as the logistic growth curve. On the other hand, it is considered to be too dependent on the inflection point of the sigmoid curves which can sometimes lead to overestimating the prediction (Gibson, Bratchell, & Roberts, 1987). The predicted model yielded the highest growth rate at 405 nm for both 5 min (μ_{max} = 1.20 h^{-1}) and 10 min (μ_{max} = 1.39 h^{-1}) treatment times, whereas the lowest growth rate was at 285 nm with μ_{max} = -4.39 h^{-1} (5 min) and μ_{max} = -0.28 h^{-1} (10 min). The treatment time also plays a major role in influencing the growth rate, which is often associated with the sigmoidal curve (Garthright, 1991). Similarly, a short lag phase was observed for 285/405 nm (λ = 2.37h; 5 min) and samples treated at 365 nm gave the longest lag phase of λ = 5.26 h (5 min) and λ = 7.39 h (10 min).

Overall the model fitting was good with RMSE values ranging from 0.01 x 10^{-2} to 1.367 x 10^{-2} for 5 min treatment, and 0.01 x 10^{-2} to 0.210 x 10^{-2} for 10 min treatment. Similarly, the model also gave R-square values of 0.99 for most treatments i.e. control, 365, 405,365/405

respectively for both time points. However, a low R-square was observed for treatment at 285 nm alone or in combination with other wavelengths due to the absence of growth (Table 1). The model accuracy and bias factors were evaluated to study the goodness of model fit. The bias factor indicates relative deviation, and the accuracy factor indicates the mean absolute ratio between the model prediction and the experimental values (Ross, 1996; Tiwari, Walsh, Rivas, Jordan, & Duffy, 2014). Overall, the model showed a good fit with BF=1 demonstrating no significant deviation from the predicted and experimental values. However, for the UV treated samples at 285 nm, a poor fit to the modified Gompertz model was observed with very high bias factor, indicating the model fit to as “fail-safe” (Ross, 1996). No significant variation was observed in relation to the accuracy factor which means that the predicted values were closer to the mean absolute ratio.

3.4. Multivariate analysis

Multivariate analysis of the most effective wavelength (285 nm) alone or its combinations (285/365/405, 285/405, 365/285 nm) on $\log_{10}$ reductions achieved for both PBS, NB and μ_{max} (h^{-1}) was carried out using principal component analysis as outlined by Metsalu and Vilo (2015). PCA score plots of three principal components (PC1, PC2 and PC3) are shown in Fig. 6, explaining 100% of variation. PC1, showed 41.1 % of variation with negative loading for μmax (-0.54), PBS (-0.71) and NB (-0.46). PC2 accounted for 33.3% of variation and showed negative loading for PBS (-0.76) and positive for μmax whereas, PC3 which accounted for 25.6% of variation showed positive loading for PBS (0.71) and negative for μmax (-0.54) and NB (-0.46). Fig. 6 a-b shows clear separation of treatment time and highlights the synergistic effect of other wavelengths.

4. Conclusion

This study demonstrates that 285 nm is the most effective wavelength which can achieve > 6 $\log_{10}$ reduction for the PBS model solution investigated. Lower inactivation rates observed in the nutrient broth model, highlight the protective effects offered by the organic media to microbial cells. Some synergistic effects were observed at lower treatment times; when combined with other wavelengths. Growth studies also demonstrated that treatment at 285 nm and its combinations resulted in no growth for *B. subtilis* cells whereas wavelength combination treatments showed some bacteriostatic effects.

Acknowledgements

This research was carried out with the financial support of the Irish Department of Agriculture, Food and the Marine.

5. References

Aihara, M., Lian, X., Shimohata, T., Uebanso, T., Mawatari, K., Harada, Y., Akutagawa, M., Kinouchi, Y., & Takahashi, A. (2014). Vegetable Surface Sterilization System Using UVA Light-Emitting Diodes. *J Med Invest, 61*, 285-290.

Akgün, M. P., & Ünlütürk, S. (2017). Effects of ultraviolet light emitting diodes (LEDs) on microbial and enzyme inactivation of apple juice. *International Journal of Food Microbiology, 260*(Supplement C), 65-74.

Baranyi, J., & Roberts, T. A. (1994). A dynamic approach to predicting bacterial growth in food. *International journal of food microbiology, 23*(3-4), 277-294.

Brem, R., Guven, M., & Karran, P. (2017). Oxidatively-generated damage to DNA and proteins mediated by photosensitized UVA. *Free Radical Biology and Medicine, 107*, 101-109.

Chevremont, A. C., Farnet, A. M., Coulomb, B., & Boudenne, J. L. (2012). Effect of coupled UV-A and UV-C LEDs on both microbiological and chemical pollution of urban wastewaters. *Science of The Total Environment, 426*(Supplement C), 304-310.

Chevremont, A. C., Farnet, A. M., Sergent, M., Coulomb, B., & Boudenne, J. L. (2012). Multivariate optimization of fecal bioindicator inactivation by coupling UV-A and UV-C LEDs. *Desalination, 285*, 219-225.

Cullen, P. J., Tiwari, B. K., & Valdramidis, V. P. (2012). Chapter 1 - Status and Trends of Novel Thermal and Non-Thermal Technologies for Fluid Foods. In P. J. Cullen, B. K. Tiwari & V. P. Valdramidis (Eds.), *Novel Thermal and Non-Thermal Technologies for Fluid Foods* (pp. 1-6). San Diego: Academic Press.

E. Fratesi, S., L. Lynch, F., L. Kirkland, B., & R. Brown, L. (2004). *Effects of SEM Preparation Techniques on the Appearance of Bacteria and Biofilms in the Carter Sandstone* (Vol. 74).

Garthright, W. E. (1991). Refinements in the prediction of microbial growth curves. *Food Microbiology, 8*(3), 239-248.

Gayán, E., Condón, S., & Álvarez, I. (2014). Biological Aspects in Food Preservation by Ultraviolet Light: a Review. *Food and Bioprocess Technology, 7*(1), 1-20.

Gibson, A. M., Bratchell, N., & Roberts, T. A. (1987). The effect of sodium chloride and temperature on the rate and extent of growth of Clostridium botulinum type A in pasteurized pork slurry. *J Appl Bacteriol, 62*(6), 479-490.

Guerrero-Beltran, J. A., & Barbosa-Canovas, G. V. (2006). Inactivation of Saccharomyces cerevisiae and polyphenoloxidase in mango nectar treated with UV light. *J Food Prot, 69*(2), 362-368.

Kim, D.-K., Kim, S.-J., & Kang, D.-H. (2017). Bactericidal effect of 266 to 279nm wavelength UVC-LEDs for inactivation of Gram positive and Gram negative foodborne pathogenic bacteria and yeasts. *Food Research International, 97*(Supplement C), 280-287.

Lui, G. Y., Roser, D., Corkish, R., Ashbolt, N. J., & Stuetz, R. (2016). Point-of-use water disinfection using ultraviolet and visible light-emitting diodes. *Science of The Total Environment, 553*, 626-635.

Metsalu, T., & Vilo, J. (2015). ClustVis: a web tool for visualizing clustering of multivariate data using Principal Component Analysis and heatmap. *43*(W1), W566-570.

Picart-Palmade, L., Cunault, C., Chevalier-Lucia, D., Belleville, M.-P., & Marchesseau, S. (2019). Potentialities and Limits of Some Non-thermal Technologies to Improve Sustainability of Food Processing. *Frontiers in Nutrition, 5*(130).

Ross, T. (1996). Indices for performance evaluation of predictive models in food microbiology. *Journal of Applied Bacteriology, 81*(5), 501-508.

Sandle, T. (2013). 11 - Other methods of sterilisation. In *Sterility, Sterilisation and Sterility Assurance for Pharmaceuticals* (pp. 157-170): Woodhead Publishing.

Song, K., Mohseni, M., & Taghipour, F. (2016). Application of ultraviolet light-emitting diodes (UV-LEDs) for water disinfection: A review. *Water Research, 94*(Supplement C), 341-349.

Song, K., Taghipour, F., & Mohseni, M. (2019). Microorganisms inactivation by wavelength combinations of ultraviolet light-emitting diodes (UV-LEDs). *Science of The Total Environment, 665*, 1103-1110.

Soni, A., Oey, I., Silcock, P., & Bremer, P. (2016). Bacillus Spores in the Food Industry: A Review on Resistance and Response to Novel Inactivation Technologies. *Comprehensive Reviews in Food Science and Food Safety, 15*(6), 1139-1148.

Tiwari, U., Walsh, D., Rivas, L., Jordan, K., & Duffy, G. (2014). Modelling the interaction of storage temperature, pH, and water activity on the growth behaviour of Listeria monocytogenes in raw and pasteurised semi-soft rind washed milk cheese during storage following ripening. *Food Control, 42*, 248-256.

The Authors declare no conflicts of interest in relation to the manuscript entitled 'Effectiveness of a novel UV light emitting diode based technology for the microbial inactivation of *Bacillus subtilis in model food systems'*

Laura Hinds

On behalf of all Authors.

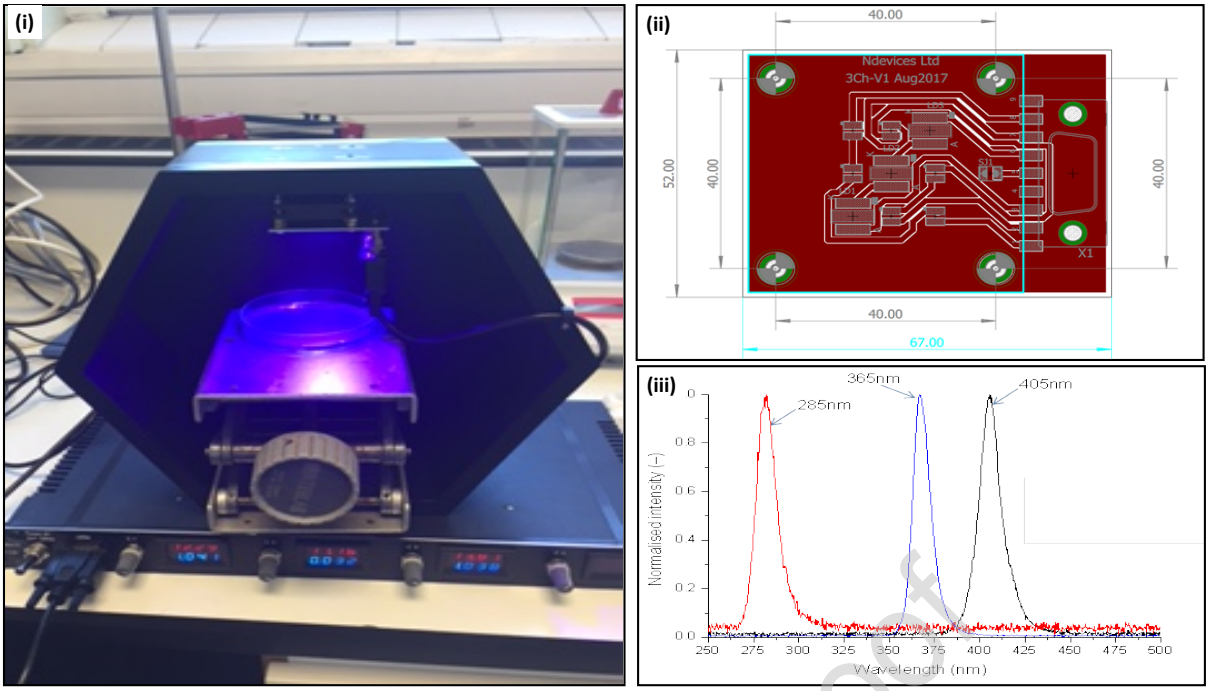

Fig 1. shows the significant aspects of the UV-LED technology device used throughout this study. It comprises of (i) a mounted LED chip with precise multichannel controller which provides digital voltage (red, Volts) and current (blue, Amps) reading for each channel with adjustable stage. (ii) The circuit board for nine LEDs (3 x 3; 285 nm, 365 nm and 405 nm) are connected in series in an optimised pattern (iii) and emission spectra for each channel were obtained using an Ocean Optics USB2000 spectrometer.

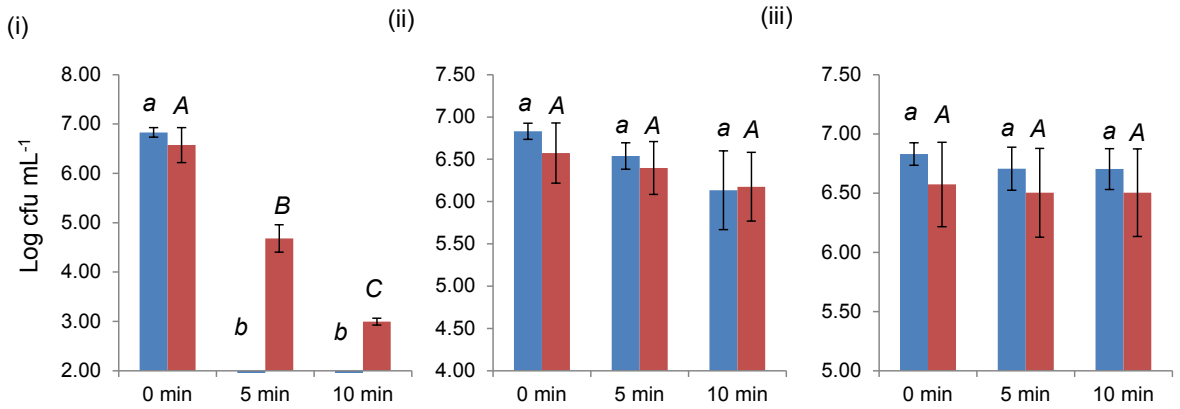

Fig. 2. Inactivation profile of *Bacillus subtilis* for treatment at individual wavelengths of (i) 285 nm; (ii) 365 nm; (ii) 405 nm for 5 and 10 min respectively (■: PBS; ■: NB). *abc Columns followed by same letter are not significantly different at P<0.05, similar for ABC.*

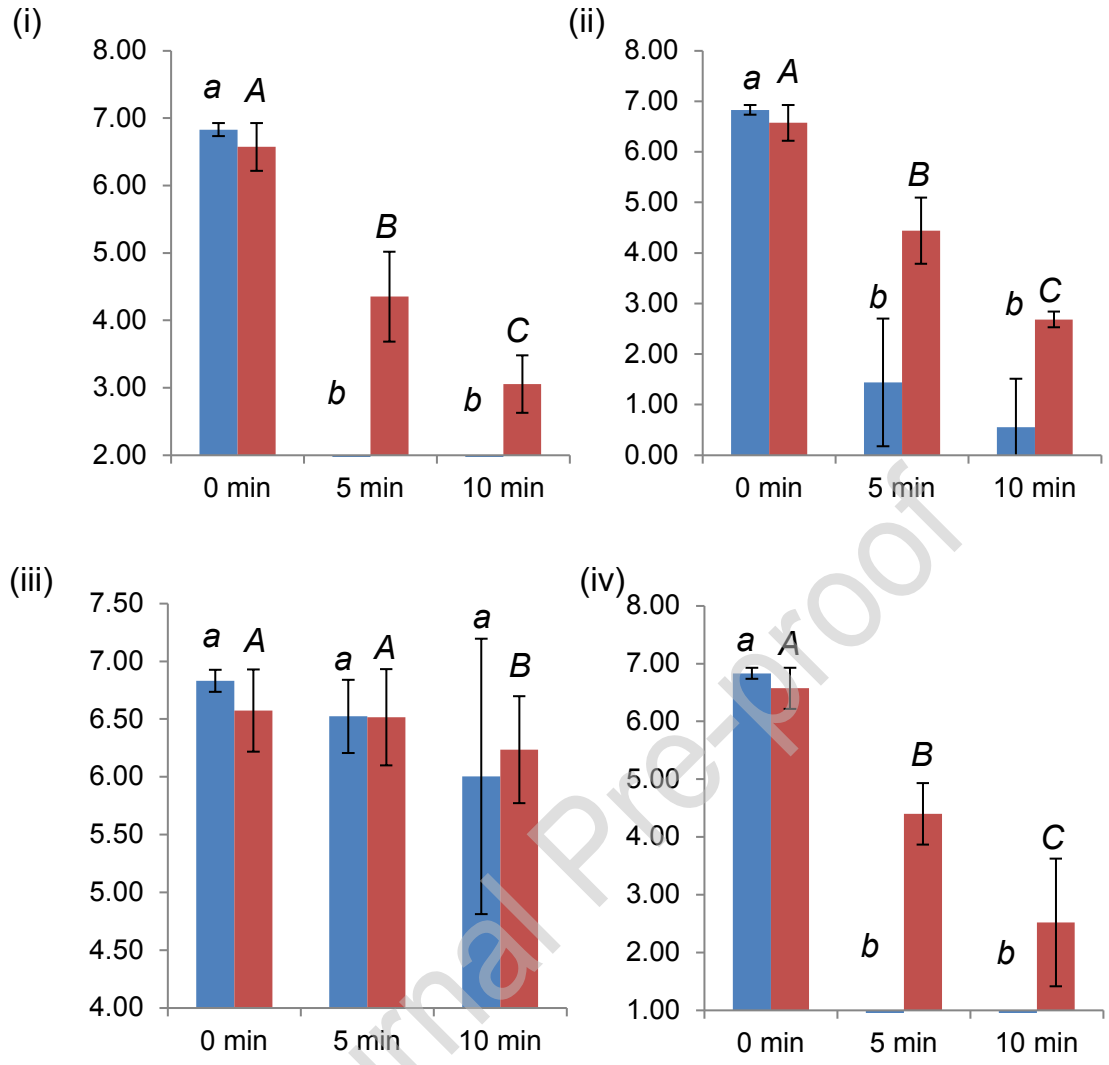

Fig. 3. Inactivation profile with of *Bacillus subtilis* for treatment at combined wavelengths of i) 285/365; (ii) 285/405; (iii)365/405 and (iv)285/365/405 for 5 and 10 min respectively (: PBS; : NB). *abc Columns followed by same letter are not significantly different at P<0.05, similar for ABC.*

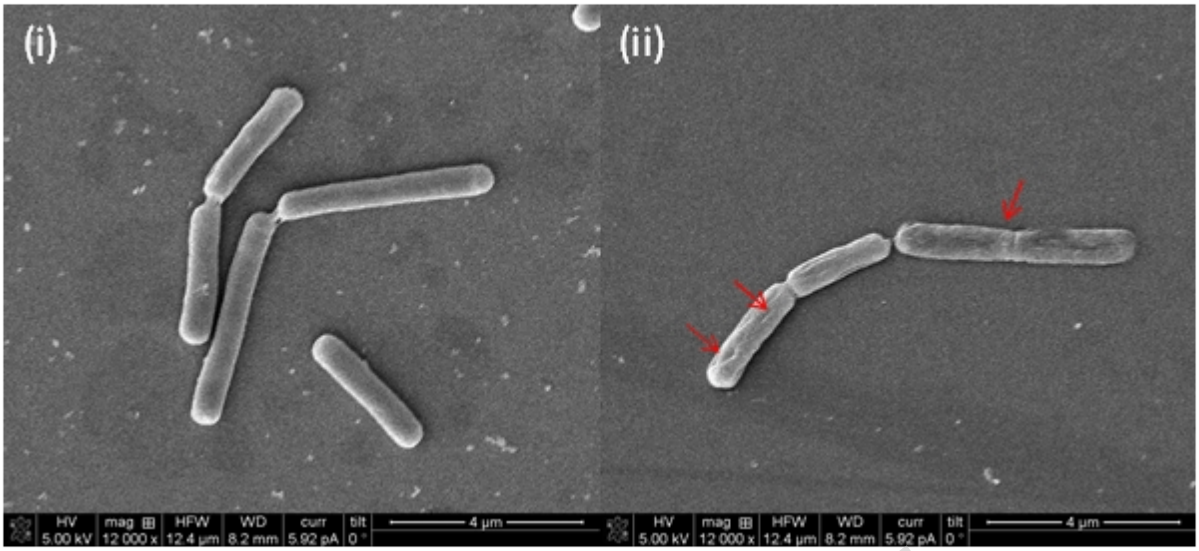

Fig. 4. Scanning electron microscopy images of Bacillus subtilis vegetative cells both pre (i) and post (ii) treatment at 285 nm.

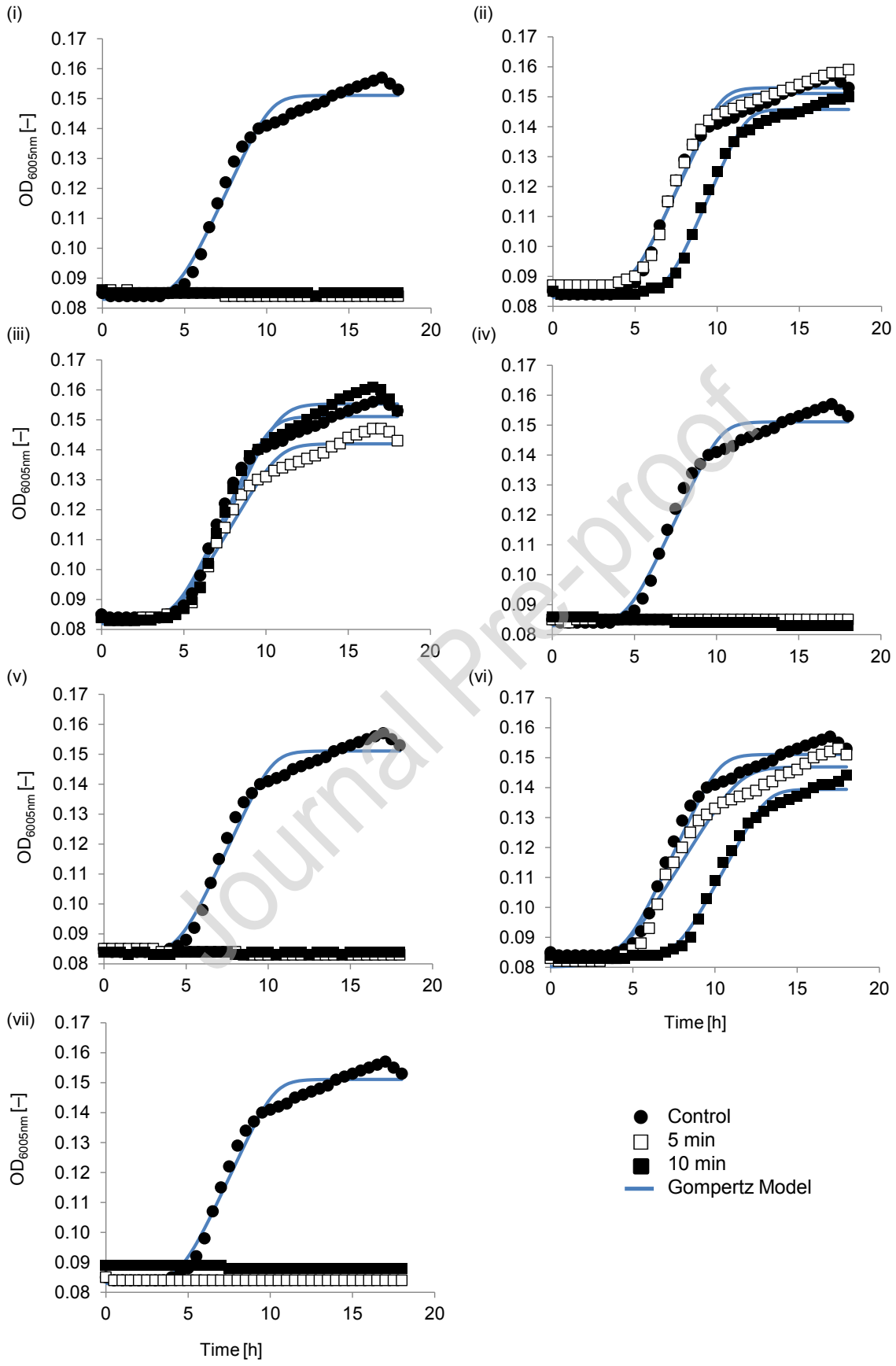

Fig.5. Growth curves for *B. subtilis* fitted to modified Gompertz model treated at (i) 285; (ii) 365; (iii) 405; (iv) 285/365; (v) 285/405; (vi)365/405 and (vii)285/365/405 nm for 5 and 10 min.

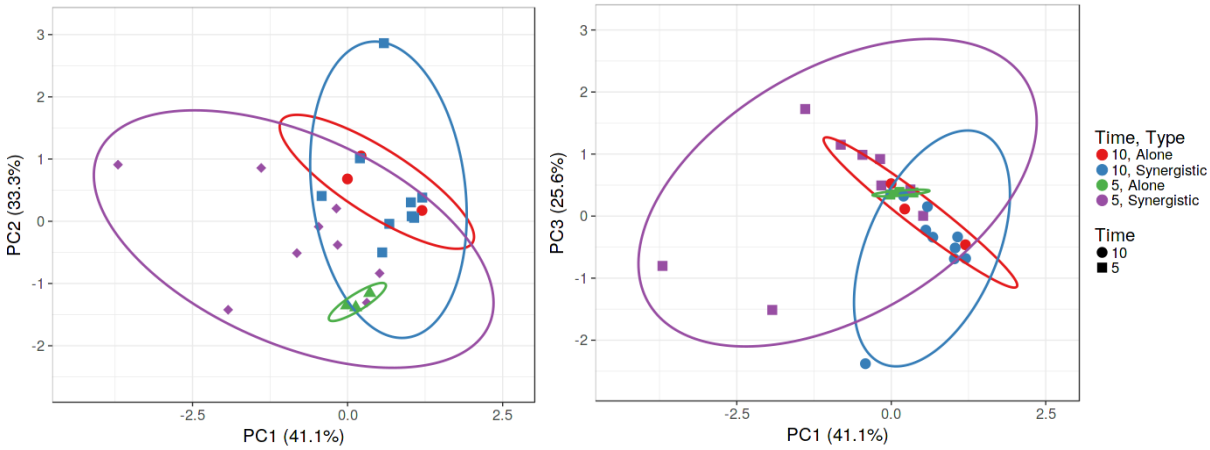

Fig. 6.Score plot of principal component analysis for a) PC1xPC2 and b) PC1xPC3 for $\log_{10}$ reductions both in PBS and NB along with μmax for samples treated at 285 nm alone or in combinations for 5 and 10 min. Prediction ellipses have probability of 0.95 for N = 24 data points.

Research highlights

1. UV treatment at 285 nm was found to be the most efficient individual wavelength for inactivation resulting in > 6 log_{10} reductions.
2. Synergistic effects were observed for 285/405 nm treatments in a nutrient broth model.
3. No bacterial growth was observed after 18 h for treatments at 285,285/365, 285/405 and 285/365/405 nm.
4. Suspended solids within a liquid medium will interfere with UV absorption and subsequently the inactivation efficiency.
5. Increasing treatment time will increase inactivation efficiency.

Table 1. *B subtilis* growth parameters along with 95% confidence interval, regression coefficient (R^2), root mean square error (RMSE) of model fit obtained for control and *treated* cells.

	μ_{max}×10^{-2} (h^{-1}) 95% Confidence Interval		**λ (h) 95% Confidence Interval**		**Bias Factor**		**Accuracy Factor**		**RMSE (×10^{-2})**		**R^2**	
	5 min	10 min	5 min	10 min	5 min	10 min	5 min	10 min	5 min	10 min	5 min	10 min
Control	1.06±0.31 (-0.03 – 2.15)	1.06±0.31 (-0.03 – 2.15)	2.90±2.00 (0.13–5.67)	2.90±2.00 (0.13–5.67)	1.007	1.007	1.001	1.001	0.193	0.193	0.99	0.99
365	1.26±0.09 (0.66 –1.85)	1.16±0.20 (0.28 –2.04)	5.26±0.54 (3.83–6.70)	7.39±0.82 (5.61–9.16)	1.005	1.003	1.001	1.000	0.174	0.101	0.99	0.99
285	-4.39±7.57 (-9.78 –1.00)	-0.28±0.24 (-1.25 –0.69)	ND	ND	23.750	1.000	1.199	1.000	1.367	0.007	0.68	0.65
405	1.20±0.31 (0.10 –2.30)	1.39±0.19 (0.52 –2.25)	4.26±0.58 (2.76–5.76)	4.18±0.62 (2.64–5.73)	1.000	1.008	1.001	1.001	0.187	0.210	0.99	0.99
365/285	-0.29±0.51 (-1.68 –1.11)	-0.17±0.23 (-1.11 –0.77)	ND	ND	1.000	1.000	1.000	1.000	0.004	0.018	0.53	0.77
285/405	-0.38±0.42 (-1.65 –0.90)	-0.01±0.01 (-0.21 –0.20)	2.37±1.74 (-0.22– 4.96)	ND	1.000	1.000	1.000	1.000	0.010	0.025	0.84	0.47

365/405	1.14±0.33 (0.02 –2.26)	1.09±0.16 (0.31 –1.88)	4.96±0.87 (3.13–6.78)	7.33±0.49 (5.96–8.70)	1.011	1.003	1.002	1.000	0.232	0.095	0.99	0.99
285/365/405	-0.44±0.00 (-0.44 –0.00)	-0.24±0.40 (-1.47 –1.00)	ND	ND	1.000	1.000	1.000	1.000	0.000	0.000	0.99	0.63